npj Aging

https://doi.org/10.1038/s41514-025-00324-y

Article in Press

Unraveling the role of polyamine metabolism in postoperative delirium: insights into biochemical mechanisms and biomarker potential

Received: 19 September 2025

Accepted: 24 December 2025

Cite this article as: Saiyed, N., Pandya, V., Pan, X. *et al.* Unraveling the role of polyamine metabolism in postoperative delirium: insights into biochemical mechanisms and biomarker potential. *npj Aging* (2026). https://doi.org/10.1038/s41514-025-00324-y

Nazia Saiyed, Vaibhav Pandya, Xiaobei Pan, Miroslava Cuperlovic-Culf, Nadia Ashrafi, Shiva Kant, Marie Migaud, Jyothi Dhuguru, Henrik Zetterberg, Bernadette McGuinness, Anthony P. Passmore, Leiv Otto Watne, Brian D. Green, Emma L. Cunningham & Stewart F. Graham

Unraveling the Role of Polyamine Metabolism in Postoperative Delirium: Insights into Biochemical Mechanisms and Biomarker Potential

Nazia Saiyed[1,2*Ψ], Vaibhav Pandya[3*], Xiaobei Pan[3], Miroslava Cuperlovic-Culf[4*], Nadia Ashrafi[1,2], Shiva Kant[5,6], Marie Migaud[7], Jyothi Dhuguru[8], Henrik Zetterberg[9-15], Bernadette McGuinness[16], Anthony P. Passmore[16], Leiv Otto Watne[17,18], Brian D. Green[3], Emma L. Cunningham[16], Stewart F. Graham[1,2,19Ψ]

1. Corewell Health East William Beaumont University Hospital, Royal Oak, MI 48073, USA

2. Corewell Health Research Institute, Metabolomics Department, Royal Oak, MI, USA.

3. Institute for Global Food Security, School of Biological Sciences, Queen's University Belfast, 19 Chlorine Gardens, Belfast, BT9 5DL, Northern Ireland.

4. Digital Technologies Research Centre, National Research Council of Canada, Ottawa, Canada.

5. Department of Radiation Oncology, Corewell Health, Royal Oak, MI, USA.

6. Department of Biology and Environmental Science, Auburn University of Montgomery, AL, USA

7. Mitchell Cancer Institute, Department of Pharmacology, Frederick P. Whiddon College of Medicine, University of South Alabama, Mobile, AL, USA.

8. Aragen Life Sciences, Number 12, Plot No 28 A, IDA, Nacharam - Mallapur Rd, Nacharam, Hyderabad, Telangana 500076.

9. Clinical Neurochemistry Laboratory, Sahlgrenska University Hospital, Mölndal, Sweden

10. Department of Neurodegenerative Disease, UCL Institute of Neurology, Queen Square, London, UK

11. UK Dementia Research Institute at UCL, London, UK

12. Hong Kong Center for Neurodegenerative Diseases, InnoHK, Hong Kong, China

13. Wisconsin Alzheimer's Disease Research Center, University of Wisconsin School of Medicine and Public Health, University of Wisconsin-Madison, Madison, WI 53792, USA

14. Centre for Brain Research, Indian Institute of Science, Bangalore, India

15. Department of Psychiatry and Neurochemistry, Institute of Neuroscience and Physiology, the Sahlgrenska Academy at the University of Gothenburg, Mölndal, Sweden

16. Centre for Public Health, Queen's University Belfast, Block B, Institute of Clinical Sciences, Royal Victoria Hospital site, Grosvenor Road, Belfast, BT12 6BA, Northern Ireland.

17. Department of Geriatric Medicine, Akershus University Hospital, Lørenskog, Norway.

18. Oslo Delirium Research Group, Institute of Clinical Medicine, Campus Ahus, University of Oslo, Oslo, Norway.

19. Oakland University-William Beaumont School of Medicine, Rochester, MI, USA.

***** Authors contributed equally

Ψ Corresponding Author:

1. Nazia Saiyed, PhD.
   Corewell Health East William Beaumont University Hospital, Corewell Health Research Institute
   3811 West 13 Mile Road, Royal Oak, MI 48073
   Office: 248-551-1089 | Fax: 248-551-2947
   Email: nazia.saiyed@corewellhealth.org

2. Stewart F Graham, PhD.
Oakland University William Beaumont School of Medicine, Corewell Health Research Institute
3811 West 13 Mile Road, Royal Oak, MI 48073
Office: 248-551-2038 | Fax: 248-551-2947
Email: stewart.graham@corewellhealth.org

Keywords: Postoperative Delirium, Polyamine Metabolism, Neuroinflammation, Urea Cycle, Oxidative Damage, Gene-Metabolite Interactions.

Running Title: Polyamine Metabolism and Postoperative Delirium: Biochemical Pathways and Biomarker Potential

Abstract:

Postoperative delirium (POD) is a common complication in older surgical patients, linked to long-term cognitive decline and progression to dementia, yet its mechanisms remain unclear. We investigated arginine-related metabolites (ARMs) in cerebrospinal fluid (CSF) from 248 patients undergoing elective-surgery: 25 developed POD. Targeted mass spectrometry, gene expression profiling, and machine learning were applied to identify metabolic predictors. POD patients showed significant correlations with citrulline, ornithine, and glutamine, while models highlighted glutamine, glutamic acid, putrescine, N1-acetylspermidine, and spermidine as key biomarkers, achieving >77% predictive accuracy. Cluster and pathway analyses revealed POD-specific shifts in GABA synthesis and polyamine metabolism, contrasting with urea cycle dominance in non-POD cases. Associations persisted after adjusting for age and CSF Aβ42. Preoperative profiles in polyamine metabolism, ammonia detoxification, and neurotransmitter regulation suggest underlying neuroinflammatory and oxidative stress vulnerabilities that reduce resilience. Targeting polyamine biosynthesis may offer novel preventative and therapeutic strategies to mitigate POD and dementia risk.

Introduction

Delirium is an acute neuropsychiatric disorder characterized by disturbances in attention, awareness, and cognition, often precipitated by acute illness, trauma, surgery, or postoperative conditions, including postoperative delirium (POD) [1, 2]. POD is common after surgery, particularly in older adults who are at high risk due to age-related vulnerabilities and comorbidities, ≥20% of high-risk patients after major surgery, and 50% to 70% of those on mechanical ventilation in critical care [3-6]. It is associated with significant healthcare costs, more nursing time per patient, longer hospital stays and higher rates of nursing home placement [7-9]. POD is also associated with longer-term negative patient outcomes, including cognitive decline, functional decline and death compared to non-postoperative delirium (NPOD) patients [10, 11].

It is unknown whether the association between POD and subsequent cognitive decline is due to underlying brain vulnerability or if the occurrence of POD itself may lead to cognitive decline independently of preoperative conditions. Several studies have indicated a potential connection between POD and neurodegeneration suggesting that patients experiencing POD may benefit from targeted opportunities to improve brain health. [3, 12, 13]. At the same time, it has been postulated that understanding and preventing POD may prevent dementia [14]. Among potential biomarkers for predicting vulnerability, arginine-related metabolites (ARMs) have garnered attention due to their involvement in neuroinflammation and vascular function, which are critical pathways in delirium and cognitive decline [15]. Whether delirium is a marker of underlying brain vulnerability, or a modifiable risk factor for dementia, the established association between POD and its associated neurodegeneration can be used to both improve patient

stratification for clinical trials and to identify novel therapeutic targets. Developing cerebrospinal fluid (CSF) biochemical markers, such as ARMs, provides a mechanistic framework to better understand preoperative delirium vulnerability that could advance research, prevention, and treatment of both delirium and dementia [16].

Previous non-targeted metabolomic profiling of CSF indicates that key metabolites in ARM pathways may be predictive of POD, highlighting its importance in the neurological basis of POD [16]. In order to further investigate the pathophysiological mechanisms underlying POD we developed a tandem mass spectrometry approach for simultaneously quantifying 18 ARMs in CSF. Then we applied this to preoperative CSF samples from patients undergoing elective surgeries, including gynecological, urological, and arthroplasty procedures. The metabolite data was reinforced by measuring the expression of genes encoding ARM pathway enzymes, to identify the underlying source of metabolic dysregulation. This integrated approach provides valuable insights into the metabolic mechanisms and pathways underlying POD, advancing our understanding of its pathophysiology and proposing polyamine metabolism as a future focus of therapeutic development.

Results:

This study used CSF to examine aberrant arginine metabolism in the brain, quantify eighteen related metabolites, assess expression of five pathway genes, involved in arginine metabolic pathway. Detailed information on the patient cohort is available in Table 1. Point biserial correlation was used to determine the relationship between POD status and all measured features (Figure 1). Although all correlation levels were low, the strongest positive correlations were with citrulline ($p=0.03$), ornithine ($p=0.03$) and glutamine ($p=0.04$) concentrations. Minor differences were observed in the projection analysis, with both PCA and t-SNE demonstrating no clear separation between the two patient groups. Statistical assessment using Wilcoxon rank-sum analysis of the first and second projections revealed no significant differences (Supplementary Figure 1). The absence of separation based on POD status was evident across the full dataset of 19 selected features and a balanced subset selected for detailed analysis. This balanced subset included all 24 patients from the POD cohort and 24 age and sex matched patients from the NPOD group. Balancing the sample sizes was essential for robust machine learning and correlation analyses, and this subset was used for subsequent investigations.

Classification using the optimized KNN method with five-fold cross-validation and validation on a balanced dataset yielded strong separation between the two patient groups. The confusion matrix for the five-fold cross-validation is shown in Figure 2A. When applied to the complete dataset, the model achieved consistent classification accuracy of 0.77 (Figure 2B). Feature importance was assessed using the SHAP method, revealing high contributions from nearly all features in the classification model. To refine

the identification of key features, we employed the following three independent feature selection methods: the Relieff machine learning algorithm, the F-test for statistical significance, and the bag-of-trees decision tree-based approach. Features consistently identified as significant across all three methods—glutamine, glutamic acid, putrescine, spermine, spermidine, and N1-acetylspermidine—were highlighted as critical markers of differentiation between the two groups (indicated in orange in Figure 2C). These results, summarized in Figure 2, demonstrate the robust performance of the KNN model and the relevance of the selected features in predicting POD. Unsupervised clustering analysis revealed distinct metabolic and gene expression patterns between POD and NPOD cohorts (Supplementary Figure 2). Hierarchical clustering (HCL) showed distinct patterns in metabolites, including GABA, ornithine, citrulline, proline, and S-adenosylmethionine (Supplementary Figure 2A and 2B). In the NPOD cohort, GAD2 and ARG1 clustered together, whereas in the delirium cohort, ARG1 clustered separately, and GAD2 was associated with ASS1. Fuzzy C-Means (FCM) clustering further highlighted these differences, especially in GABA's association with urea cycle and polyamine pathway metabolites (Supplementary Figure 2 and 2D).

Pairwise relationships and data-driven networks for the two groups were evaluated using distance correlation analysis (Figure 3). This method identifies both linear and nonlinear as well as monotonic and non-monotonic correlations, providing a comprehensive view of interdependencies between features. To account for the influence of sample size, balanced sample groups were used as previously described. Figures 3A and 3C highlight strong correlations with p-values below 0.01 and correlation coefficients exceeding 0.5. The analysis revealed preserved correlations in some feature pairs across

both groups, whereas notable differences emerged in metabolite-metabolite, gene-gene, and gene-metabolite interactions. For instance, GABA exhibited significant shifts in its correlation network between the two cohorts. In the NPOD group, GABA was primarily associated with proline, spermidine, and agmatine, but these correlations were absent in the POD group. Instead, GABA formed strong associations with putrescine, N1-acetylspermine, and N8-acetylspermidine in the POD cohort. Proline also demonstrated a significant network shift in the POD group, gaining correlations with multiple features, including all studied genes. Signed distance correlation analysis further identified a low, nonsignificant negative correlation trend between GABA and proline, complementing the observed changes (Figure 3C). Overall, this correlation analysis underscores shifts in metabolic and gene expression networks associated with POD, offering insights into the underlying pathophysiological mechanisms. Figure 3A and 3B illustrate these significant differences, emphasizing the altered interplay of key features in the POD group.

To further explore changes in the role of each feature within the network of measured variables, we compared pairwise correlation values for each feature across the two groups. Figure 4 presents a linear regression analysis of these pairwise correlations. On the x-axis, each data point represents the distance correlation value for a feature in the NPOD cohort, whereas the y-axis corresponds to its correlation value in the POD group. The slope of the regression line quantifies the alignment of correlations between the two groups. A slope of 1 indicates identical correlations in both groups, whereas a negative slope suggests significant shifts in feature relationships. Among the metabolites, GABA exhibited the most pronounced change, with a strongly negative slope. Similarly, features such as N1-acetylspermine, N8-acetylspermidine, arginase 1, and glutamate

decarboxylase 2 also demonstrated notable negative slopes, indicating substantial alterations in their correlation networks. These findings, summarized in Figure 4, reveal significant changes in the metabolic and gene interaction networks in patients predisposed to POD. The observed shifts in correlation patterns for key features highlight their potential involvement in the disrupted metabolic interactions associated with delirium.

Determined changes in clusters and correlations are shown in the pathway schematic in Figure 5. It is apparent from this analysis that the GABA synthesis pathway has a stronger association with polyamines in POD patients. Moreover, in the NPOD group, the relationship is much more apparent with metabolites of the urea cycle. Figure 5 outlines the pathological mechanisms underlying delirium observed in postoperative patients, as evidenced by abnormalities in CSF.

Discussion:

Taken together, our results suggest that nitrogen metabolism appears reorganized within the central nervous system (CNS) or possibly reflects systemic metabolic differences mirrored in CSF among patients prone to POD. This is evidenced by altered metabolic pathways, including a shift from urea cycle activity in NPOD patients to a stronger association with the GABA-polyamine axis in POD patients. This highlights the central role of the arginine metabolic pathway in regulating arginine fate and suggests associations consistent with mechanisms that may contribute to delirium vulnerability. Specifically, our pathway analysis reveals that in POD patients, the association between GABA synthesis and polyamine metabolism is markedly stronger than in NPOD patients, where the urea cycle dominates nitrogen metabolism. These findings suggest that disruptions in neurotransmitter synthesis pathways, such as GABA production, and altered ammonia detoxification may drive the pathophysiology of delirium. While our results delineate a coherent biochemical pattern, they remain associative; causal inferences require longitudinal or interventional validation. The observed significant positive correlations between citrulline, ornithine, and glutamine further implicate disruptions in the ammonia detoxification process [24]. Ammonia accumulation, may interfere with neurotransmitter synthesis and homeostasis, potentially contributing to delirium onset [24, 25]. Reduced Aβ42 is known to impair synaptic function and may exacerbate disruptions in nitrogen metabolism by amplifying neuroinflammatory processes, leading to further dysregulation of ammonia detoxification and neurotransmitter imbalance [26]. These results align with prior studies [27-29] emphasizing the role of altered arginine metabolism in delirium vulnerability and extend

this understanding by pinpointing specific metabolic and genetic pathways associated with POD. Our findings highlight potential therapeutic targets, such as modulation of the GABA-polyamine axis and enhancement of ammonia detoxification pathways, to mitigate delirium risk and its progression to cognitive decline

Across all analytical platforms employed here glutamine, glutamic acid, putrescine, spermine, spermidine and N1-acetylspermidine were consistently altered. These polyamine-related metabolites are critical markers differentiating POD from NPOD groups. Polyamine metabolism has been linked to dementia onset and its involvement in POD warrants further investigation and there is future potential for exploitation in diagnosis or therapy.

Citrulline and ornithine are central components of the urea cycle, a critical metabolic pathway responsible for detoxifying ammonia in the liver by converting it into urea, which is subsequently excreted in urine [30, 31]. In this metabolic pathway, ornithine is regenerated, while citrulline is synthesized from ornithine and carbamoyl phosphate in a reaction catalyzed by the enzyme ornithine transcarbamylase [24]. The significant positive correlation of citrulline and ornithine with POD suggests a potential disruption in the urea cycle, impairing ammonia detoxification [32, 33]. This impairment may lead to elevated ammonia levels capable of crossing the blood-brain barrier, and disrupt neurotransmission, contributing to the cognitive disturbances observed in delirium [32, 34]. These findings align with previous research indicating that hyperammonemia can cause alterations in brain function and is associated with hepatic encephalopathy, a condition characterized by confusion and disorientation similar to delirium [12, 35, 36]. Further investigations are warranted to confirm whether these correlations reflect direct

metabolite accumulation or secondary metabolic adaptations in POD patients. Glutamine is a nonessential amino acid playing a pivotal role in nitrogen metabolism, acting as a carrier of ammonia in a nontoxic form [37, 38]. A significant positive correlation was observed between glutamine levels in POD, indicating that elevated glutamine may be associated with the condition. This suggests that disruptions in nitrogen balance and neurotransmitter cycling could contribute to the observed symptoms of delirium [39]. Further supporting this, machine learning approaches, identified glutamine and its downstream product, glutamic acid, as significant biomarkers of POD. Glutamine is converted to glutamic acid, an excitatory neurotransmitter, through the action of glutaminase [40]. Glutamic acid is also a precursor for GABA, an inhibitory neurotransmitter crucial for maintaining neural excitatory-inhibitory balance. The positive association of glutamine and glutamic acid in patients experiencing POD may indicate an imbalance in neurotransmitter levels, potentially leading to the neural hyperexcitability observed in delirium [41, 42]. Furthermore, glutamine's role in the synthesis of both excitatory and inhibitory neurotransmitters underscores its importance in maintaining cognitive function, and its dysregulation may be a contributing factor to the cognitive decline associated with delirium [41, 43]. The disruption of glutamine-glutamate cycling, particularly under conditions of metabolic stress, could impair GABA synthesis, contributing to the neurochemical disturbances observed in delirium and potentially accelerating cognitive decline in ADRD [41, 44].

In contrast, $A\beta_{42}$ showed a significant negative correlation with POD. Reduced Aβ42 levels, often associated with impaired clearance and amyloid pathology, may influence arginine metabolism by altering NO production, which is essential for vascular

and neuronal function [45]. Additionally, disruptions in polyamine synthesis mediated by arginine derived metabolites like ornithine and citrulline, could contribute to neuroinflammatory and excitotoxic processes, further exacerbating cognitive dysfunction [26]. The interplay between Aβ42 and arginine metabolism may thus reflect a broader metabolic imbalance that contributes to neuronal vulnerability in conditions like delirium.

Machine learning methods identified polyamines such as putrescine, N1-acetylspermidine, spermine, spermidine as significant biomarkers of POD. Spermidine, spermine, and putrescine, the principal polyamines in human tissues, were consistently altered in POD patients, highlighting their potential role in the interplay between polyamine metabolism, oxidative stress, and neuroinflammatory vulnerability [16]. These small organic cations play essential roles in cellular function, including DNA stabilization, protein synthesis, and ion-channel regulation. [46, 47], and are synthesized from arginine via arginase and ornithine decarboxylase [47]. Because polyamine metabolism is systemic, alterations in peripheral or hepatic polyamine flux may influence CNS polyamine levels via transport and metabolic coupling across the blood-brain barrier [31, 41, 48]. When dysregulated, polyamine oxidation by amine oxidases generates hydrogen peroxide and reactive aldehydes that intensify oxidative and inflammatory stress within the CNS [49, 50]. These reactions may compromise membrane integrity and blood brain barrier function, fostering immune cell infiltration and sustained neuroinflammation. Such processes could underlie the acute cognitive dysfunction characteristic of delirium and its potential progression toward Alzheimer's-type neurodegeneration[50]. These processes not only contribute to acute cognitive impairments in delirium but also link altered

polyamine metabolism to the neurodegenerative processes observed in ADRD, including the formation of neurofibrillary tangles and amyloid plaques [12, 51].

Additionally, polyamines are intricately tied to the urea cycle through their synthesis from ornithine [52]. An overproduction of polyamines in delirium may divert ornithine away from ammonia detoxification, exacerbating hyperammonemia, a state strongly correlated with disrupted neurotransmitter balance and neurotoxicity [25]. Elevated levels of polyamines also interact with NMDA receptors on microglia, triggering calcium influx, microglial activation, and subsequent production of pro-inflammatory cytokines such as TNF-α, IL-1β, and IL-6 [48, 53-61]. These inflammatory processes are further amplified by the activation of NF-κB and the generation of peroxynitrite through nitric oxide synthase (iNOS) activity, perpetuating a cycle of neuroinflammation and cellular damage [62-65]. Collectively, these findings suggest that altered polyamine metabolism not only exacerbates oxidative and inflammatory pathways but also disrupts neurotransmitter regulation, forming a multifaceted mechanism underlying the onset and progression of delirium as summarized in Figure 5 [48, 53, 66, 67]. This new mechanistic understanding proposes polyamines as a target for therapeutic intervention, where modulating their levels or inhibiting their oxidation could reduce the risk of delirium and its progression to ADRD [50, 53]. At the same time, polyamine metabolism exerts context-dependent effects: while excessive accumulation or oxidation can amplify oxidative stress and inflammatory cascades, moderate activation of polyamine biosynthesis or supplementation has been reported to enhance autophagy, synaptic resilience, and cognitive performance during aging [47, 68, 69]. Thus, polyamine modulation may also

represent a potential strategy to preserve cognitive function during aging, underscoring its dual role in neurodegeneration and neuroprotection.

We conducted a linear regression analysis to compare feature correlations between two patient groups. Negative slopes for GABA, N1-acetylspermine, N8-acetylspermidine, arginase 1, and glutamate decarboxylase 2 indicate significant shifts in their correlation networks, suggesting altered metabolic interactions in delirium patients. GABA is the primary inhibitory neurotransmitter in the central nervous system, regulating neuronal excitability and preventing overexcitation. It is synthesized from glutamic acid by the enzyme glutamate decarboxylase, which is encoded by the GAD2 gene [70-72]. The significant changes in GABA correlation networks between POD and NPOD patients suggest a disruption in inhibitory neurotransmission in POD individuals [73]. A decrease in GABAergic signaling can lead to neuronal hyperexcitability, a condition that has been linked to cognitive disturbances and the development of neuropsychiatric disorders [74, 75]. The disruption of GABAergic signaling in delirium may thus contribute to the cognitive symptoms observed in these patients, as well as the potential progression to dementia. The negative slope observed for GABA and its altered correlations with putrescine, N1-Aspd, and N8-aspd suggest that polyamine dysregulation might disrupt normal GABAergic function [76, 77]. As polyamines such as spermidine, putrescine, and spermine affect NMDA receptors and other signaling pathways, they may contribute to GABA dysfunction through impaired interactions with glutamate, leading to neuronal excitability and cognitive dysfunction [26, 77, 78]. This altered GABA network may indicate a loss of inhibitory control that can lead to the hyperexcitability observed in delirium.

ARG1 is an enzyme in the urea cycle that converts arginine into ornithine and urea [79, 80]. GLUL, also known as glutamine synthetase, catalyzes the ATP-dependent conversion of glutamate and ammonia into glutamine, playing a crucial role in nitrogen metabolism and detoxification [79, 81].The significant alterations in ARG1 and GLUL gene expression and their correlation networks in delirium-prone patients highlight the disruption of ammonia detoxification and nitrogen metabolism in these individuals [79, 81]. Impaired activity of these enzymes can lead to the accumulation of toxic ammonia levels, contributing to the neural dysfunction observed in delirium. These findings further underscore the importance of the arginine metabolic pathway in the pathophysiology of POD [82-84].

A critical connection between polyamines and ammonia detoxification is suggested by the observed correlations between ornithine and citrulline. Elevated levels of these metabolites in delirium-prone individuals likely reflect a bottleneck in the urea cycle, suggesting impaired ammonia detoxification. Polyamines, synthesized from ornithine, may be favored over the urea cycle, creating a diversion of metabolic flux. This could result in hyperammonemia, contributing to the neurotoxic effects observed in delirium.

The analysis of these correlation networks reveals a cascade of disruptions in metabolic processes. Polyamine overproduction, coupled with impaired ammonia handling, exacerbates oxidative stress and neuroinflammation, which are key contributors to both acute delirium and long-term cognitive decline in Alzheimer's disease and other neurodegenerative conditions. The changes in the correlation networks of GABA, N1-acetylspermine, N8-acetylspermidine, arginase 1, and glutamate decarboxylase

2 highlight a systemic alteration in neurochemical balance that promotes cognitive dysfunction. The integration of polyamine metabolism, ammonia detoxification, and neurotransmitter regulation underscores the complex interactions that drive delirium and potentially contribute to its progression to ADRD. Targeting these pathways could hold therapeutic promise for preventing or mitigating both the acute and chronic cognitive effects of delirium. Additionally, our approach using 400 µL for gene expression in cerebrospinal fluid represents the first study of its kind, demonstrating the potential for minimally invasive techniques in neurodegenerative disease research.

There is scope for future POD studies to go further. Additionally, differences in recruitment, diagnostic approach, and peri-operative management between the Belfast and Oslo cohorts may have introduced unmeasured variation. Although all analyses were adjusted for age and CSF biomarkers (Aβ42, t-tau, and p-tau), potential confounding from anesthesia type, peri-operative medications, or postoperative care cannot be excluded. The study design here meant that it was not possible to explore the immediate pathophysiological changes occurring during a delirium episode. In the Oslo cohort, postoperative delirium was identified solely from retrospective review of clinical notes. While the same diagnostic framework was applied, this approach may have introduced a degree of uncertainty and should be regarded as a limitation of the study. Longitudinal studies are needed to validate the findings and predict long-term cognitive outcomes. Although several statistically significant findings were observed, larger sample sizes are needed to determine generalizability. Further research will be needed to understand the causal relationships of metabolic shifts and to test the proposed therapeutic strategies.

Our methodical analysis of ARM metabolism implicates polyamines, including putrescine, spermidine, and spermine, in the pathophysiology of POD. Dysregulation of these polyamines may serve as an early indicator of delirium risk and contribute to neuroinflammation and cognitive decline. We detected perturbations in key metabolic pathways, such as the urea cycle and neurotransmitter regulation, which further underscore a shift in metabolic interactions in patients prone to POD. These findings provide novel insights into the molecular mechanisms connecting polyamine metabolism and delirium. Although the study does not explore the immediate pathophysiological mechanisms during delirium episodes, it offers novel insights into the metabolic shifts in delirium patients. Future longitudinal studies are needed to validate these findings and explore how polyamine dysregulation could predict long-term cognitive outcomes.

Methods

Study Design

Study participants were recruited from Belfast and Oslo, with detailed cohort information provided in Table 1 and Supplementary Table 2. The study was approved by the Office for Research Ethics Committees Northern Ireland (REC reference: 10/NIR01/5, protocol number: 09069PP-OPMS) and the Regional Committee for Ethics in Medical Research in Norway (REC 2011/2052). It was conducted in accordance with the Declaration of Helsinki, and all participants provided written informed consent. The study included 248 participants aged 65 years or older, comprising 138 individuals from Belfast and 110 from Oslo. All participants were scheduled for primary elective surgeries, which included hip and knee arthroplasties, as well as gynecological and urological procedures such as transurethral resection of the prostate (TURP) and transurethral resection of bladder tumor (TURB) for benign conditions. Participants with a pre-existing diagnosis of dementia or other neurodegenerative conditions were excluded from the study. Both the Belfast and Oslo cohorts included assessments of demographic variables (age, gender, and education) and baseline cognitive function using the Mini-Mental State Examination (MMSE). Biomarker evaluations were performed for apolipoprotein E (APOE) genotype, amyloid-beta (Aβ1-42), total tau (t-tau), and phosphorylated tau 181 (p-tau). POD was diagnosed in the Belfast cohort using the Confusion Assessment Method (CAM). POD was diagnosed in the Belfast cohort using the Confusion Assessment Method (CAM) administered on post-operative days 1, 2 and 3 and supported by subsequent retrospective comprehensive review of the notes. [17]. In the Oslo cohort, POD diagnosis was determined solely through retrospective comprehensive examination of case notes.

Detailed information on these variables is presented in Table 1 and Supplementary Table 2. The study design for the Belfast and Oslo cohort has been previously published [16-18]

Sample Collection and Processing

CSF collection and handling followed previously published standardized procedures for both cohorts. In Belfast CSF was sampled prior to spinal anesthesia, as described by Pan et al. (2019) [16] and Cunningham et al. (2019) [18]. Samples were centrifuged at 2000 × g for 10 min at 4 °C, aliquoted into polypropylene tubes, and stored at −80 °C. The Oslo cohort used identical processing conditions except the samples were centrifuged at room temperature as detailed by Idland et al. (2020) [17].

Sample Preparation for Liquid Chromatography-Mass Spectrometry (LC-MS)

The synthesis and characterization of agmatine derivatives have been previously published [19]. Samples were prepared using a direct dilution and filtration method. In brief, 8 µL of labeled internal standard (IS) mix (keeping the final IS concentration at 100 nM) was added to 10 µL of CSF. The IS mix contained $^{13}C_6$-arginine (CK Isotopes CLM-2265-H), D_4-citrulline (DLM-6039), D_6-ornithine (LGC TRC-O695553), D_8-putrescine (TRC-D416027), D_8-spermidine (DLM-9261), D_8-spermine (DLM-9262), D_3-creatine (DLM-1302), $^{13}C_6$ $^{15}N_4$-argininosuccinate (CNLM-9007), D_3-aspartate (DLM-546), D_5-glutamate (DLM-556), ^{15}N-proline (NLM-835), D_6-N^1-acetylspermidine (TRC-A187847), D_3-N^8-acetylspermidine (TRC-A188002), D_3-N^1-acetylspermine (TRC-A188007), D_3-S-adenosylmethionine (TRC-A291532), D_3-5′-methylthioadenosine (TRC-D242602), ^{15}N-GABA (TRC-A602922), and ^{15}N-glutamine (NLM-1016). The volume was adjusted to 400 µL by adding 382 µL of 10% MeOH (with 0.1% formic acid) and mixed well. Subsequently,

the solution was passed through a 3.0 kDa cutoff Nanosep filter following the manufacturer's instructions (Pall Corporation, NY, USA). After collecting the filtrate, 50 µL was transferred to an LC-MS vial for analysis. To assess sample recovery, an analyte mix was spiked into the samples to a final concentration of 100 nM.

Development of the Targeted LC-MS Method

The analyses were performed using a Sciex 5500+ QTRAP-ready triple quadrupole mass spectrometer equipped with a turbo ion source coupled to an ultra high-performance liquid chromatography (UHPLC) system (AB Sciex ExionLC Systems, Foster City, CA, USA). Initially, individual ARMs were directly infused into standard solutions (1.0 µg mL-1 in ultrapure water) to determine the optimum collision energy, declustering potential, and collision cell exit potential. The stable transitions (quantifier and qualifier) for each analyte were determined. For quantification, an 11-point calibration curve for each analyte was prepared, ranging from 0.5 nM to 1.0 µM. Chromatographic separations were performed on an X-select HSS T3 column (300 Å; 3.5 µm; 4.6 × 100 mm, Waters Inc. Milford, MA, USA). The mobile phase consisted of ultrapure water with 0.1% formic acid (solvent A) and methanol (MeOH) with 0.1% formic acid (solvent B). The standardized gradient UHPLC elution program was as follows: 0-2 min, 0% A; 2-10 min, 5% B; 11-13 min, 90% B; 14 min, 100% B; 14-16 min, 0% B. The column temperature was held constant at 30°C, and the sample chamber temperature was set at 8°C.

The mass spectrometry settings were as follows: positive polarity with an ion spray voltage fixed at 5.0 kV, the heater gas (GS2, N2) heated to 500°C, collision gas (CAD) value set at 9.0, nebulizer gas (GS1, N2) at 14.0 units, and the entrance potential set at 10 V. The samples were introduced into the source post-column separation through

UHPLC at a flow rate of 0.3 mL/min. Mass spectra were recorded and processed with the Analytics software (Sciex OS). Peak areas for the analytes were also calculated using this software. For each concentration, area values were recorded in triplicate, and the average area and standard error were calculated.

Assay Validation

The multiple reaction monitoring (MRM) method was developed and validated following the latest M10 ICH harmonized guidelines under FDA-2019-D-1469. The specificity and selectivity of the assay were evaluated by examining the chromatogram of standard and IS-spiked samples to ensure consistency in retention time and transitions. The sensitivity of the LC-MS/MS method was determined by assessing the signal-to-noise ratio (S/N) of each analyte, and the limit of detection (LOD) and lower limit of quantification (LLOQ) were measured based on peak areas four and ten times greater than the S/N ratio, respectively.

To check for any carry-over effect, a 'blank run' was analyzed after three injections of high levels of QC samples. The concentrations of each analyte used to create the calibration curves were 0.5, 1.0, 2.0, 5.0, 10, 20, 50, 100, 200, 500, 700, and 1000 nM. IS (100 nM) was used along with labeled ARMs. The acceptance criteria for each concentration for all the analytes were set at ±15% of the expected values at CAL points and ±20% of the expected values at LLOQ for each analyte. The concentrations used to prepare the QC samples were: 8.0 nM (LQC), 150 nM (MQC), and 750 nM (HQC). These samples were analyzed along with standards in sets of five replicates (n = 5) over three days. To assess precision, a percentage relative standard deviation value (% RSD) of the expected QC concentration was calculated for each analyte. The recovery for all the

analytes and IS was estimated by comparing the analyte concentration in CSF-extracted QCs with blank extracts spiked with labeled analytes post-extraction. The matrix effect was determined by comparing the peak area for each analyte concentration of QC post-extraction against the standard analyte prepared in 10% MeOH. The acceptance criteria for calculating any potential matrix effect were set at ±15% of QC concentration. If the observed peak area fell within this range, it was considered that there was no matrix effect.

Gene Expression Study

The selected genes for analysis were arginase 1 (ARG1), argininosuccinate synthase 1 (ASS1), glutamate-ammonia ligase (GLUL), glutamate decarboxylase 2 (GAD2), and spermine N1-acetyltransferase 1 (SAT1) from Integrated DNA Technologies (IDT; Coralville, IA, USA, Primer details added in Supplementary table 3). Total RNA was extracted from 400µl of CSF using the Qiagen miRNeasy Serum/Plasma Kit (Cat: 217184, Qiagen, Hilden, Germany) according to the manufacturer's instructions. To ensure reliable and consistent data, RNA spike-ins from Tataa Biocenter (RS25S, TATAA Biocenter, Göteborg, Sweden) were used as internal controls for data normalization and to account for any variations in RNA input, isolation efficiency, and reverse transcription. Isolated RNA was transcribed into complementary DNA (cDNA) using the iScript cDNA Synthesis Kit (Cat: 1708891, BIO-RAD, Hercules, California, USA), followed by a pre-amplification step using the PreAmp Master Mix (Cat: 1725160, BIO-RAD, Hercules, CA, USA) to enhance the detection sensitivity of low-abundance transcripts. Quantification of target gene expression levels was carried out using quantitative PCR (qPCR) with the SYBR Green Supermix (Cat: 1725270, BIO-RAD Hercules, CA, USA) and interplate

calibration (generated in-house) for each plate, running the qPCR reactions on a Via7 Real-Time PCR Detection System (Applied Biosystems, Foster City, CA, USA). Amplification conditions were established based on the manufacturer's guidelines (BIO-RAD, Hercules, CA, USA). Data analysis was performed using the comparative Ct (ΔΔCt) method, with normalization against the RNA spike-ins to ensure accurate and reliable results. Future studies should incorporate measurement of corresponding enzyme activities or protein concentrations in CSF to complement transcript level observations.

Optimized MRM parameters for all ARM analytes and labelled compounds are provided in Supplementary Table 1. The observed results suggested that electrospray ionization (ESI) along with MRM in positive mode provides a high degree of selectivity for ARMs. The reference values for HCDs in CSF were determined by analyzing 248 samples. Supplementary Table 2 provides a comprehensive summary of these findings, including the concentrations of 19 metabolites, expression levels of five genes from qPCR, and patient characteristics, consolidating all relevant data into a single resource. Samples were processed and analyzed without access to any identifying information or characteristics, ensuring unbiased data collection and analysis.

Data Preprocessing

Samples with more than 50% missing values in either the gene expression or metabolite panels were excluded, and imputation was applied only to features with less than 50% missingness. Out of the initial samples, 170 remained for further analysis. Values below the level of detection were imputed using 1/5th of the minimum value measured in all samples for that feature [20]. Subsequently, the data underwent logarithmic transformation (log2) for all further analysis. We conducted data analysis

using principal component analysis (PCA) and t-distributed stochastic neighbor embedding (t-SNE). In both cases, we used Wilcoxon rank sum statistical analysis to show the statistical differences between groups [21]. We corrected the separation of results based on the three sample collection groups using Combat [22].

Normalization and Batch Correction

Normalization aimed to reduce technical variation and ensure comparability across samples. Metabolite intensity values were scaled measure-wise, using autoscaling. Batch effect adjustment was performed using the ComBat function from the sva R package (v3.42.0). The effectiveness of autoscaling and ComBat batch correction was verified by visual inspection of PCA plots before and after correction, confirming removal of site-specific variance and consistent clustering of quality control samples.

Data Analysis

Correlations were calculated using distance and point biserial correlation. The distance correlation was performed using previously published applications [23]. To assess potential confounding, surgery type (arthroplasty, gynecologic, or urologic) was included as a covariate in all linear models and statistical analyses; its inclusion did not materially alter model outcomes or the significance of identified metabolites. All procedures included in this study were elective and non-oncologic. No participants underwent surgeries related to active malignancy, minimizing potential confounding from tumor-associated polyamine metabolism.

Feature Selection

We used machine learning methods such as Relieff (rank importance of predictors using the ReliefF or RReliefF algorithm) and bagging of trees as well as univariate feature ranking using F-tests (FSRFT), to select the most significantly different features between different groups of samples. The data was first transformed using log2 and then autoscaled (z-score normalized) for each feature before analysis. In Relieff and bagging of trees, all features with positive weight are considered to possibly contribute to group selection. In the F-test, features with a p-value below 0.05 are considered significant and kept for further analysis.

Machine Learning Model

A predictive model for POD was developed using a machine learning from all 19 features. The model was built using optimizable KNN (*k*-nearest neighbor classification) in Matlab, with Bayesian optimization of hyperparameters for the best classification accuracy. The optimal hyperparameters for POD classification were found to be Hamming distance, two neighbors, inverse distance weight, and standardized data. The analysis was performed using five fold cross-validation and a separate validation set of 10 samples. The balanced dataset, comprising 24 POD and 24 age and sex matched NPOD samples, for robust machine learning and correlation analysis for subsequent investigations.

Data Availability:

This study is registered and archived at the NIH Common Fund's National Metabolomics Data Repository (Metabolomics Workbench, Study ID ST004212; DOI http://dx.doi.org/10.21228/M8G55V). Data are available through the Metabolomics Workbench portal (https://www.metabolomicsworkbench.org), supported by NIH grant U2C-DK119886 and OT2-OD030544.

Acknowledgments:

This work was funded by NIH/NIA grants (NIA/R21/R21AG067083 and (NIA/R33/R33AG067083) under the program: Clarifying the Relationship between Delirium and Alzheimer's Disease and Related Dementias', Belfast Trust Charitable funds and Belfast Arthroplasty Research Trust. LOW is funded by the South-Eastern Norway Regional Health Authorities (# 2017095), the Norwegian Health Association (#19536, #1513) and by Wellcome Leap's Dynamic Resilience Program (jointly funded by Temasek Trust) (#104617). We express our gratitude to the John and Marilyn Bishop Charitable Foundation for their generous contributions. Their support has been invaluable in making this work possible. HZ is a Wallenberg Scholar and a Distinguished Professor at the Swedish Research Council supported by grants from the Swedish Research Council (#2023-00356, #2022-01018 and #2019-02397), the European Union's Horizon Europe research and innovation program under grant agreement No 101053962, Swedish State Support for Clinical Research (#ALFGBG-71320), the National Institute for Health and Care Research University College London Hospitals Biomedical Research Centre, the UK Dementia Research Institute at UCL (UKDRI-1003), and an anonymous donor.

Author Contributions

The authors contributed to the study as follows: SFG, ELG, BDG and LOW contributed to conceptualization, study design, supervision, project administration, funding acquisition, and critical manuscript review. NS was responsible for conceptualization, manuscript drafting, data collection, statistical analysis, experimental work, data analysis, data interpretation, manuscript revision, methodology development, visualization, and critical manuscript review. VP participated in data collection, experimental work, methodology development, and review. MCC contributed to conceptualization, statistical and machine learning analysis, data interpretation, visualization, and review. HZ, BM, APP, and XP contributed to data analysis and visualization. NA contributed to visualization and review. SK was involved in experimental work, data interpretation, and review. MM and JD contributed to data curation and review. All authors have read, reviewed and agreed to the published version of the manuscript.

Conflicts of Interest: HZ has served at scientific advisory boards and/or as a consultant for Abbvie, Acumen, Alector, Alzinova, ALZpath, Amylyx, Annexon, Apellis, Artery Therapeutics, AZTherapies, Cognito Therapeutics, CogRx, Denali, Eisai, Enigma, LabCorp, Merry Life, Nervgen, Novo Nordisk, Optoceutics, Passage Bio, Pinteon Therapeutics, Prothena, Quanterix, Red Abbey Labs, reMYND, Roche, Samumed, Siemens Healthineers, Triplet Therapeutics, and Wave, has given lectures sponsored by Alzecure, BioArctic, Biogen, Cellectricon, Fujirebio, Lilly, Novo Nordisk, Roche, and WebMD, and is a co-founder of Brain Biomarker Solutions in Gothenburg AB (BBS), which is a part of the GU Ventures Incubator Program (outside submitted work).

Abbreviations:

Aβ42: Amyloid beta 42
Agm: Agmatine
ARG1: Arginase 1
ASS1: Argininosuccinate synthase 1
CIT: Citrulline
Cr: Creatine
D: Aspartic acid (aspartate)
E: Glutamic acid (glutamate)
GABA: Gamma-aminobutyric acid
GLUL: Glutamate-ammonia ligase
MMSE: Mini-Mental State Examination test score
N1Aspr: N1-acetylspermine
N1AspD: N1-acetylspermidine
N8AspD: N8-acetylspermidine
Orn: Ornithine
Pro: Proline
Put: Putrescine
Q: Glutamine
RS: Arginine
SAM: S-Adenosyl methionine
SAT1: Spermine N1-acetyltransferase 1
SpD: Spermidine
Spr: Spermine
t-tau: Total tau
p-tau: Phosphorylated tau

References

[1] Wilson JE, Mart MF, Cunningham C, Shehabi Y, Girard TD, MacLullich AMJ, Slooter AJC, Ely EW (2020) Delirium. *Nat Rev Dis Primers* **6**, 90.

[2] Urbánek L, Urbánková P, Satinský I, Trávníček T, Penka I, Hruda J (2023) Postoperative delirium. *Rozhl Chir* **102**, 381-386.

[3] Vasunilashorn SM, Lunardi N, Newman JC, Crosby G, Acker L, Abel T, Bhatnagar S, Cunningham C, de Cabo R, Dugan L, Hippensteel JA, Ishizawa Y, Lahiri S, Marcantonio ER, Xie Z, Inouye SK, Terrando N (2023) Preclinical and translational models for delirium: Recommendations for future research from the NIDUS delirium network. **19**, 2150-2174.

[4] Robinson TN, Eiseman B (2008) Postoperative delirium in the elderly: diagnosis and management. *Clin Interv Aging* **3**, 351-355.

[5] Inouye SK, Marcantonio ER, Kosar CM, Tommet D, Schmitt EM, Travison TG, Saczynski JS, Ngo LH, Alsop DC, Jones RN (2016) The short-term and long-term relationship between delirium and cognitive trajectory in older surgical patients. *Alzheimers Dement* **12**, 766-775.

[6] Scott JE, Mathias JL, Kneebone AC (2015) Incidence of delirium following total joint replacement in older adults: a meta-analysis. *Gen Hosp Psychiatry* **37**, 223-229.

[7] Caplan GA, Teodorczuk A, Streatfeild J (2020) The financial and social costs of delirium. **11**, 105-112.

[8] Pezzullo L, Streatfeild J (2019) Economic impact of delirium in Australia: a cost of illness study. **9**, e027514.

[9] Inouye SK, Westendorp RG, Saczynski JS (2014) Delirium in elderly people. *Lancet* **383**, 911-922.

[10] Krogseth M, Davis D, Jackson TA, Zetterberg H, Watne LO, Lindberg M, Chitalu P, Tsui A, Selbæk G, Wyller TB (2023) Delirium, neurofilament light chain, and progressive cognitive impairment: analysis of a prospective Norwegian population-based cohort. *Lancet Healthy Longev* **4**, e399-e408.

[11] Tsui A, Searle SD, Bowden H, Hoffmann K, Hornby J, Goslett A, Weston-Clarke M, Howes LH, Street R, Perera R, Taee K, Kustermann C, Chitalu P, Razavi B, Magni F, Das D, Kim S, Chaturvedi N, Sampson EL, Rockwood K, Cunningham C, Ely EW, Richardson SJ, Brayne C, Terrera GM, Tieges Z, MacLullich A, Davis D (2022) The effect of baseline cognition and delirium on long-term cognitive impairment and mortality: a prospective population-based study. *Lancet Healthy Longev* **3**, e232-e241.

[12] Fong TG, Inouye SK (2022) The inter-relationship between delirium and dementia: the importance of delirium prevention. *Nat Rev Neurol* **18**, 579-596.

[13] Subramaniyan S, Terrando N (2019) Neuroinflammation and Perioperative Neurocognitive Disorders. *Anesth Analg* **128**, 781-788.

[14] Williams ST (2013) Pathophysiology of encephalopathy and delirium. *J Clin Neurophysiol* **30**, 435-437.

[15] Fleszar MG, Wiśniewski J, Zboch M, Diakowska D, Gamian A, Krzystek-Korpacka M (2019) Targeted metabolomic analysis of nitric oxide/L-arginine pathway metabolites in dementia: association with pathology, severity, and structural brain changes. *Scientific Reports* **9**, 13764.

[16] Pan X, Cunningham EL (2019) Cerebrospinal Fluid Spermidine, Glutamine and Putrescine Predict Postoperative Delirium Following Elective Orthopaedic Surgery. **9**, 4191.

[17] Idland AV, Sala-Llonch R, Watne LO, Brækhus A, Hansson O, Blennow K, Zetterberg H, Sørensen Ø, Walhovd KB, Wyller TB, Fjell AM (2020) Biomarker profiling beyond amyloid and tau: cerebrospinal fluid markers, hippocampal atrophy, and memory change in cognitively unimpaired older adults. *Neurobiol Aging* **93**, 1-15.
[18] Cunningham EL, McGuinness B, McAuley DF, Toombs J, Mawhinney T, O'Brien S, Beverland D, Schott JM, Lunn MP, Zetterberg H, Passmore AP (2019) CSF Beta-amyloid 1-42 Concentration Predicts Delirium Following Elective Arthroplasty Surgery in an Observational Cohort Study. *Ann Surg* **269**, 1200-1205.
[19] Dhuguru J, Migaud ME (2022) 1-(4-Aminobutyl)guanidine. *Molbank* **2022**, M1463.
[20] Giskeødegård GF, Lydersen S (2022) Measurements below the detection limit. *Tidsskr Nor Laegeforen* **142**.
[21] Salem D, Surendra A, McDowell GS, Čuperlović-Culf M (2024) Projection Statistics – ProST: Online statistical assessment of group separation in data projection analysis. *bioRxiv*, 2024.2009.2004.611273.
[22] Zhang Y, Parmigiani G (2020) ComBat-seq: batch effect adjustment for RNA-seq count data. **2**, lqaa078.
[23] Monti F, Stewart D, Surendra A, Alecu I, Nguyen-Tran T (2023) Signed Distance Correlation (SiDCo): an online implementation of distance correlation and partial distance correlation for data-driven network analysis. **39**.
[24] Couchet M, Breuillard C, Corne C, Rendu J, Morio B, Schlattner U, Moinard C (2021) Ornithine Transcarbamylase - From Structure to Metabolism: An Update. *Front Physiol* **12**, 748249.
[25] Huang SS (2022) Hyperammonemia-Associated Delirium Mimics Dementia: A Case Report. *Psychiatry Clin Psychopharmacol* **32**, 181-183.
[26] Ju YH, Bhalla M, Hyeon SJ, Oh JE, Yoo S, Chae U, Kwon J, Koh W, Lim J, Park YM, Lee J, Cho IJ, Lee H, Ryu H, Lee CJ (2022) Astrocytic urea cycle detoxifies Aβ-derived ammonia while impairing memory in Alzheimer's disease. *Cell Metab* **34**, 1104-1120.e1108.
[27] Jung M, Pan X, Cunningham EL, Passmore AP, McGuinness B (2022) The Influence of Orthopedic Surgery on Circulating Metabolite Levels, and their Associations with the Incidence of Postoperative Delirium. **12**.
[28] Xiao MZ, Liu CX, Zhou LG, Yang Y, Wang Y (2023) Postoperative delirium, neuroinflammation, and influencing factors of postoperative delirium: A review. **102**, e32991.
[29] Han Y, Zhang W, Liu J, Song Y, Liu T, Li Z, Wang X, Yang N, Li Y, Han D, Mi X, Zhou Y, Li M, Guo X, Zhong L, Wang G, Yuan Y (2020) Metabolomic and Lipidomic Profiling of Preoperative CSF in Elderly Hip Fracture Patients With Postoperative Delirium. *Front Aging Neurosci* **12**, 570210.
[30] Wang H, Ran J, Jiang T (2014) Urea. *Subcell Biochem* **73**, 7-29.
[31] Morris SM, Jr. (2002) Regulation of enzymes of the urea cycle and arginine metabolism. *Annu Rev Nutr* **22**, 87-105.
[32] Simpson KL, MacLeod EL, Kakajiwala A, Gropman AL, Ah Mew N (1993) Urea Cycle Disorders Overview In *GeneReviews(®)*, Adam MP, Feldman J, Mirzaa GM, Pagon RA, Wallace SE, Amemiya A, eds. University of Washington, Seattle

[33] Walker V (2009) Ammonia toxicity and its prevention in inherited defects of the urea cycle. *Diabetes Obes Metab* **11**, 823-835.
[34] Gropman AL, Summar M, Leonard JV (2007) Neurological implications of urea cycle disorders. *J Inherit Metab Dis* **30**, 865-879.

[35] Cheon SY, Song J (2022) Novel insights into non-alcoholic fatty liver disease and dementia: insulin resistance, hyperammonemia, gut dysbiosis, vascular impairment, and inflammation. **12**, 99.
[36] Ribas GS, Lopes FF, Deon M, Vargas CR (2022) Hyperammonemia in Inherited Metabolic Diseases. **42**, 2593-2610.
[37] Cruzat V, Macedo Rogero M (2018) Glutamine: Metabolism and Immune Function, Supplementation and Clinical Translation. **10**.
[38] Häussinger D, Schliess F (2007) Glutamine metabolism and signaling in the liver. *Front Biosci* **12**, 371-391.
[39] Fan YY, Luo RY, Wang MT, Yuan CY, Sun YY, Jing JY (2024) Mechanisms underlying delirium in patients with critical illness. *Front Aging Neurosci* **16**, 1446523.
[40] (!!! INVALID CITATION !!!).
[41] Andersen JV, Schousboe A, Verkhratsky A (2022) Astrocyte energy and neurotransmitter metabolism in Alzheimer's disease: Integration of the glutamate/GABA-glutamine cycle. *Prog Neurobiol* **217**, 102331.
[42] Czapski GA, Strosznajder JB (2021) Glutamate and GABA in Microglia-Neuron Cross-Talk in Alzheimer's Disease. **22**.
[43] Dong XX, Wang Y, Qin ZH (2009) Molecular mechanisms of excitotoxicity and their relevance to pathogenesis of neurodegenerative diseases. *Acta Pharmacol Sin* **30**, 379-387.
[44] Aldana BI, Zhang Y, Jensen P, Chandrasekaran A, Christensen SK, Nielsen TT, Nielsen JE, Hyttel P, Larsen MR, Waagepetersen HS, Freude KK (2020) Glutamate-glutamine homeostasis is perturbed in neurons and astrocytes derived from patient iPSC models of frontotemporal dementia. **13**, 125.
[45] Akama KT, Albanese C, Pestell RG, Van Eldik LJ (1998) Amyloid beta-peptide stimulates nitric oxide production in astrocytes through an NFkappaB-dependent mechanism. *Proc Natl Acad Sci U S A* **95**, 5795-5800.
[46] Arthur R, Jamwal S, Kumar P (2024) A review on polyamines as promising next-generation neuroprotective and anti-aging therapy. *European Journal of Pharmacology* **978**, 176804.
[47] Sagar NA, Tarafdar S (2021) Polyamines: Functions, Metabolism, and Role in Human Disease Management. **9**.
[48] Pegg AE (2009) Mammalian polyamine metabolism and function. *IUBMB Life* **61**, 880-894.
[49] Benkő P, Gémes K, Fehér A (2022) Polyamine Oxidase-Generated Reactive Oxygen Species in Plant Development and Adaptation: The Polyamine Oxidase-NADPH Oxidase Nexus. **11**.
[50] Tönnies E, Trushina E (2017) Oxidative Stress, Synaptic Dysfunction, and Alzheimer's Disease. *J Alzheimers Dis* **57**, 1105-1121.
[51] Nasb M, Tao W, Chen N (2024) Alzheimer's Disease Puzzle: Delving into Pathogenesis Hypotheses. *Aging Dis* **15**, 43-73.
[52] Oratz M, Rothschild MA, Schreiber SS, Burks A, Mongelli J, Matarese B (1983) The role of the urea cycle and polyamines in albumin synthesis. *Hepatology* **3**, 567-571.
[53] Sandusky-Beltran LA, Kovalenko A, Ma C, Calahatian JIT, Placides DS, Watler MD, Hunt JB, Darling AL, Baker JD, Blair LJ, Martin MD, Fontaine SN, Dickey CA, Lussier AL, Weeber EJ, Selenica M-LB, Nash KR, Gordon MN, Morgan D, Lee DC (2019) Spermidine/spermine-N1-acetyltransferase ablation impacts tauopathy-induced polyamine stress response. *Alzheimer's Research & Therapy* **11**, 58.
[54] Subramaniam S, O'Connor MJ, Masukawa LM, McGonigle P (1994) Polyamine effects on the NMDA receptor in human brain. *Exp Neurol* **130**, 323-330.

[55] Smith JA, Das A, Ray SK, Banik NL (2012) Role of pro-inflammatory cytokines released from microglia in neurodegenerative diseases. *Brain Res Bull* **87**, 10-20.
[56] Wang WY, Tan MS, Yu JT, Tan L (2015) Role of pro-inflammatory cytokines released from microglia in Alzheimer's disease. *Ann Transl Med* **3**, 136.
[57] Minogue AM, Barrett JP, Lynch MA (2012) LPS-induced release of IL-6 from glia modulates production of IL-1β in a JAK2-dependent manner. *J Neuroinflammation* **9**, 126.
[58] Dheen ST, Kaur C, Ling EA (2007) Microglial activation and its implications in the brain diseases. *Curr Med Chem* **14**, 1189-1197.
[59] Eyo UB, Peng J, Swiatkowski P, Mukherjee A, Bispo A, Wu LJ (2014) Neuronal hyperactivity recruits microglial processes via neuronal NMDA receptors and microglial P2Y12 receptors after status epilepticus. *J Neurosci* **34**, 10528-10540.
[60] Salvi M, Toninello A (2004) Effects of polyamines on mitochondrial Ca(2+) transport. *Biochim Biophys Acta* **1661**, 113-124.
[61] Miao J, Ma H, Yang Y, Liao Y, Lin C, Zheng J, Yu M, Lan J (2023) Microglia in Alzheimer's disease: pathogenesis, mechanisms, and therapeutic potentials. *Front Aging Neurosci* **15**, 1201982.
[62] Maréchal A, Mattioli TA, Stuehr DJ, Santolini J (2007) Activation of peroxynitrite by inducible nitric-oxide synthase: a direct source of nitrative stress. *J Biol Chem* **282**, 14101-14112.
[63] Saini R, Singh S (2019) Inducible nitric oxide synthase: An asset to neutrophils. *J Leukoc Biol* **105**, 49-61.
[64] Pacher P, Beckman JS, Liaudet L (2007) Nitric oxide and peroxynitrite in health and disease. *Physiol Rev* **87**, 315-424.
[65] Lull ME, Block ML (2010) Microglial activation and chronic neurodegeneration. *Neurotherapeutics* **7**, 354-365.
[66] Pernet V, Bourgeois P, Di Polo A (2007) A role for polyamines in retinal ganglion cell excitotoxic death. *J Neurochem* **103**, 1481-1490.
[67] Murray Stewart T, Dunston TT, Woster PM, Casero RA, Jr. (2018) Polyamine catabolism and oxidative damage. *J Biol Chem* **293**, 18736-18745.
[68] Arthur R, Jamwal S, Kumar P (2024) A review on polyamines as promising next-generation neuroprotective and anti-aging therapy. *Eur J Pharmacol* **978**, 176804.
[69] Sandusky-Beltran LA, Kovalenko A, Ma C, Calahatian JIT, Placides DS, Watler MD, Hunt JB, Darling AL, Baker JD, Blair LJ, Martin MD, Fontaine SN, Dickey CA, Lussier AL, Weeber EJ, Selenica MB, Nash KR, Gordon MN, Morgan D, Lee DC (2019) Spermidine/spermine-N(1)-acetyltransferase ablation impacts tauopathy-induced polyamine stress response. **11**, 58.
[70] Pan ZZ (2012) Transcriptional control of Gad2. *Transcription* **3**, 68-72.
[71] Petroff OA (2002) GABA and glutamate in the human brain. *Neuroscientist* **8**, 562-573.
[72] Kim JI, Ganesan S, Luo SX, Wu YW, Park E, Huang EJ, Chen L, Ding JB (2015) Aldehyde dehydrogenase 1a1 mediates a GABA synthesis pathway in midbrain dopaminergic neurons. *Science* **350**, 102-106.
[73] Li XY, Zhang SY, Hong YZ, Chen ZG, Long Y, Yuan DH, Zhao JJ, Tang SS, Wang H, Hong H (2024) TGR5-mediated lateral hypothalamus-dCA3-dorsolateral septum circuit regulates depressive-like behavior in male mice. *Neuron* **112**, 1795-1814.e1710.
[74] Maestú F, de Haan W, Busche MA, DeFelipe J (2021) Neuronal excitation/inhibition imbalance: core element of a translational perspective on Alzheimer pathophysiology. *Ageing Res Rev* **69**, 101372.
[75] Govindpani K, Calvo-Flores Guzmán B, Vinnakota C, Waldvogel HJ, Faull RL, Kwakowsky A (2017) Towards a Better Understanding of GABAergic Remodeling in Alzheimer's Disease. *Int J Mol Sci* **18**.

[76] Lim J, Bhalla M, Park MG, Koh W, Lee CJ (2023) Putrescine acetyltransferase (PAT/SAT1) dependent GABA synthesis in astrocytes. *bioRxiv*, 2023.2005.2015.540086.
[77] Cervelli M, Averna M (2022) The Involvement of Polyamines Catabolism in the Crosstalk between Neurons and Astrocytes in Neurodegeneration. **10**.
[78] Kovács Z, Skatchkov SN, Veh RW, Szabó Z, Németh K, Szabó PT, Kardos J, Héja L (2021) Critical Role of Astrocytic Polyamine and GABA Metabolism in Epileptogenesis. *Front Cell Neurosci* **15**, 787319.
[79] Adeva MM, Souto G, Blanco N, Donapetry C (2012) Ammonium metabolism in humans. *Metabolism* **61**, 1495-1511.
[80] Sin YY, Baron G, Schulze A, Funk CD (2015) Arginase-1 deficiency. *J Mol Med (Berl)* **93**, 1287-1296.
[81] Caldwell RW, Rodriguez PC, Toque HA, Narayanan SP, Caldwell RB (2018) Arginase: A Multifaceted Enzyme Important in Health and Disease. *Physiol Rev* **98**, 641-665.
[82] Cherry JD, Olschowka JA, O'Banion MK (2014) Neuroinflammation and M2 microglia: the good, the bad, and the inflamed. *J Neuroinflammation* **11**, 98.
[83] Ellwardt E, Zipp F (2014) Molecular mechanisms linking neuroinflammation and neurodegeneration in MS. *Exp Neurol* **262 Pt A**, 8-17.
[84] Mahajan UV, Varma VR, Griswold ME, Blackshear CT (2020) Dysregulation of multiple metabolic networks related to brain transmethylation and polyamine pathways in Alzheimer disease: A targeted metabolomic and transcriptomic study. **17**, e1003012.

Figure Legends:

Figure 1. Univariate overview of the data.

The figure shows the relationship between post-operative delirium (POD) and various measured factors (A). The point biserial correlation was used to examine how each factor was related to the occurrence of POD. Two analyses were performed: one on the original data (A) and another after applying a batch correction to reduce any systematic error (B). The data was transformed using a log2 scale before statistical testing to ensure accurate comparison. (C) The chart presents the absolute values for all factors considered in the analysis. These factors are categorized based on whether the patient experienced POD or not. The normal range of each factor is indicated by a reference line, helping to highlight whether a factor is within the expected range or showing abnormalities.

Figure 2. KNN classification model.

(A) The confusion matrix from five-fold cross-validation and validation sets demonstrates the model's ability to correctly classify post-operative delirium (POD) patients and NPOD patients, highlighting the performance of the KNN model.
(B) The AUC-ROC curve reflects the model’s overall accuracy, assessing how well it distinguishes between the two patient groups by plotting true positive rates against false positive rates.(C) Key features that significantly differentiate the patient groups are highlighted in orange, emphasizing their relevance in predicting the occurrence of postoperative delirium. These features play a crucial role in the model's predictive power.

Figure 3. Correlation Analysis.

Data were log2 transformed and auto scaled prior to correlation analysis. (A) Distance correlation was calculated for patients experiencing POD and matching set of patients that do not experience POD, using a threshold of p-value < 0.01 and distance correlation value > 0.5. (B) Pearson calculation was computed for the same group. (C) Distance

correlation is calculated for each patient group as in (A). (D) Pearson calculation was computed for the same group. The distance correlation (A & C) is multiplied by the sign of the Pearson correlation (B & D) indicating the correlation direction trend.

Figure 4. Comparison between overall correlations of each measured feature with all other features in two groups of samples through linear regression analysis.

Slope of 1 (S=1) indicates perfect agreement between correlations with all other features in two sample groups; deviation from slope of 1 indicates level of difference in correlation for a given feature between two patient cohorts. Negative slopes for GABA, N1-Aspd, N8-Aspd, ARG1 and GAD2 suggest significant changes in their correlation networks, reflecting altered metabolic interactions in delirium-prone patients.

Figure 5. Schematic representation of significant pathways involving the analyzed metabolites and genes.

This figure outlines the pathological mechanisms underlying delirium observed in postoperative patients, as evidenced by abnormalities in cerebrospinal fluid. Overactive polyamine metabolism elevates concentrations of putrescine, spermidine, and spermine, which bind to and activate NMDA receptors on neuronal dendrites. This activation triggers an excessive influx of calcium ions (Ca^{2+}), initiating a cascade of downstream events. These include the upregulation of proinflammatory cytokines (TNFα, IL-1β, IL-6), which exacerbate neuronal stress, impair ammonia clearance, and promote urea accumulation, further increasing neurotoxicity. Concurrently, mitochondrial dysfunction leads to the accumulation of reactive oxygen species (ROS). Together, these molecular disturbances, neuronal dysfunction, oxidative stress, and inflammatory imbalances, drive the onset of

delirium, illustrating a cascade of metabolic and inflammatory impairments that may underlie disease progression.

Table:

Table 1: Characteristics of the total sample set and significant subgroups in patients with NPOD and POD. Data include the distribution of samples by sex (Male/Female), type of surgery performed (hip/knee), and key clinical and demographic parameters. These parameters encompass the Mini Mental State Examination (MMSE) score (mean ± SD), years in education (mean ± SD), cerebrospinal fluid (CSF) biomarkers including Aβ42, p-tau, and t-tau (mean ± SD), as well as the p-tau/Aβ42 ratio. Values are presented for the total cohort and stratified into NPOD and POD subgroups to highlight significant differences.

	NPOD	POD	p-value (NPOD v.s. POD)
Samples Male/Female	64/82	12/12	
Age at surgery, mean (SD)	73.9(6.01)	77.3(6.76)	0.01
Type of surgery: Orthopedic (knee/hip replacement).	74/70 (2 no info.)	17/7	
Mini Mental State Examination Score, mean (SD)	27.5(2.31)	27.0(2.0)	0.21
Years in Education, mean (SD)	12.1(2.76)	11(2.6)	0.10
CSF AB42, mean (SD)	610.8(227.69)	475.6(231.07)	0.01
CSF p-tau, mean (SD)	54.1(22.61)	51.3(24.06)	0.61
CSF t-tau, mean (SD)	314.8(164.10)	312(177.03)	0.88
p-tau/AB42 ratio	0.1(0.07)	0.1(0.08)	0.08

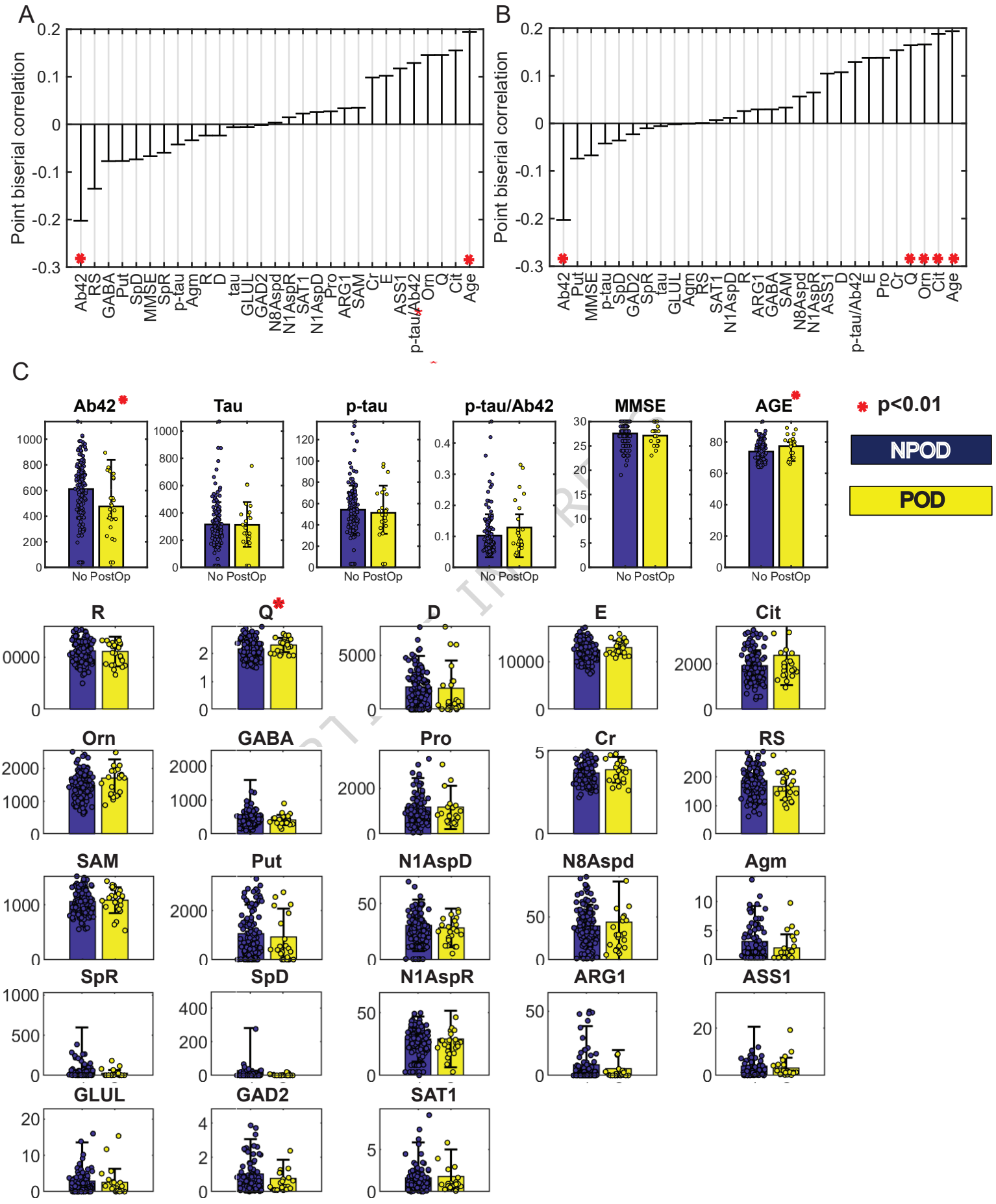
A
Point biserial correlation
0.2
0.1
0
-0.1
-0.2
-0.3
Ab42
RS
GABA
Put
SpD
MMSE
SpR
p-tau
Agm
R
D
tau
GLUL
GAD2
N8Aspd
N1AspR
SAT1
N1AspD
Pro
ARG1
SAM
Cr
E
ASS1
p-tau/Ab42
Orn
Q
Cit
Age
B
Point biserial correlation
Ab42
Put
MMSE
p-tau
SpD
GAD2
SpR
tau
GLUL
Agm
RS
SAT1
N1AspD
R
ARG1
GABA
SAM
N8Aspd
N1AspR
ASS1
D
p-tau/Ab42
E
Pro
Cr
Q
Orn
Cit
Age
C
Ab42
Tau
p-tau
p-tau/Ab42
MMSE
AGE
No PostOp
p<0.01
NPOD
POD
R
Q
D
E
Cit
Orn
GABA
Pro
Cr
RS
SAM
Put
N1AspD
N8Aspd
Agm
SpR
SpD
N1AspR
ARG1
ASS1
GLUL
GAD2
SAT1

A

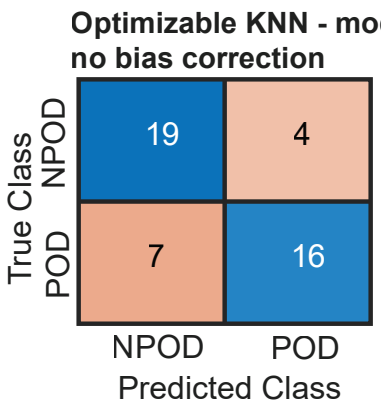

B

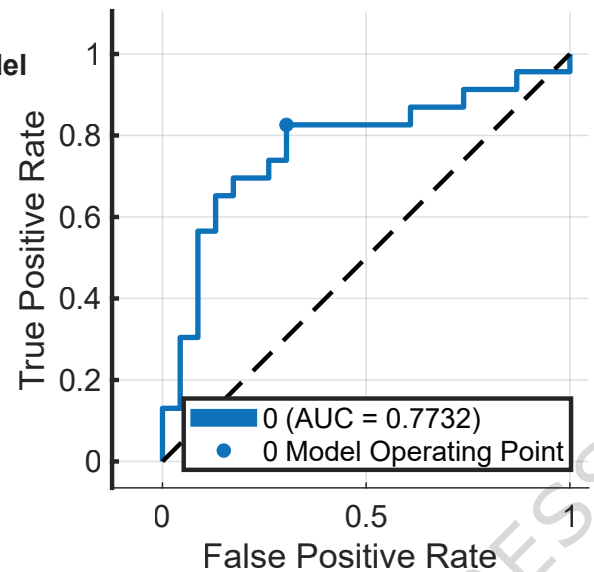

C

	Relieff (weight>0)	fsrf (p<0.05)	RF (weight>0)
R	-3.2E-04	2.8E-05	3.7E-02
Q	5.1E-03	7.8E-03	1.5E-01
D	-5.5E-03	3.3E-01	-4.2E-02
E	1.1E-02	2.3E-02	1.1E-01
Cit	-1.3E-03	3.0E-02	-1.1E-02
Orn	6.6E-03	3.7E-01	1.1E-02
GABA	1.2E-03	3.7E-01	7.1E-02
Pro	-6.2E-03	7.6E-01	-5.3E-02
Cr	-1.3E-02	9.3E-01	-4.5E-02
RS	-2.3E-03	2.0E-01	-3.7E-02
SAM	-1.6E-03	2.0E-02	-1.7E-02
Put	1.2E-02	5.2E-02	5.9E-02
N1AspD	7.0E-03	1.9E-03	1.3E-02
N8Aspd	-2.9E-03	5.2E-02	-6.1E-02
Agm	-9.1E-03	2.6E-02	-2.8E-02
SpR	2.2E-03	1.5E-12	3.4E-01
SpD	5.5E-03	3.7E-20	1.0E-01
N1AspR	3.6E-03	5.0E-02	-1.5E-02
ARG1	-8.0E-03	7.6E-02	2.8E-02
ASS1	-1.7E-03	5.2E-02	-3.4E-05
GLUL	-9.4E-03	8.8E-01	-7.2E-02
GAD2	-1.2E-03	1.5E-01	1.9E-02
SAT1	-4.7E-03	8.6E-02	-7.0E-02

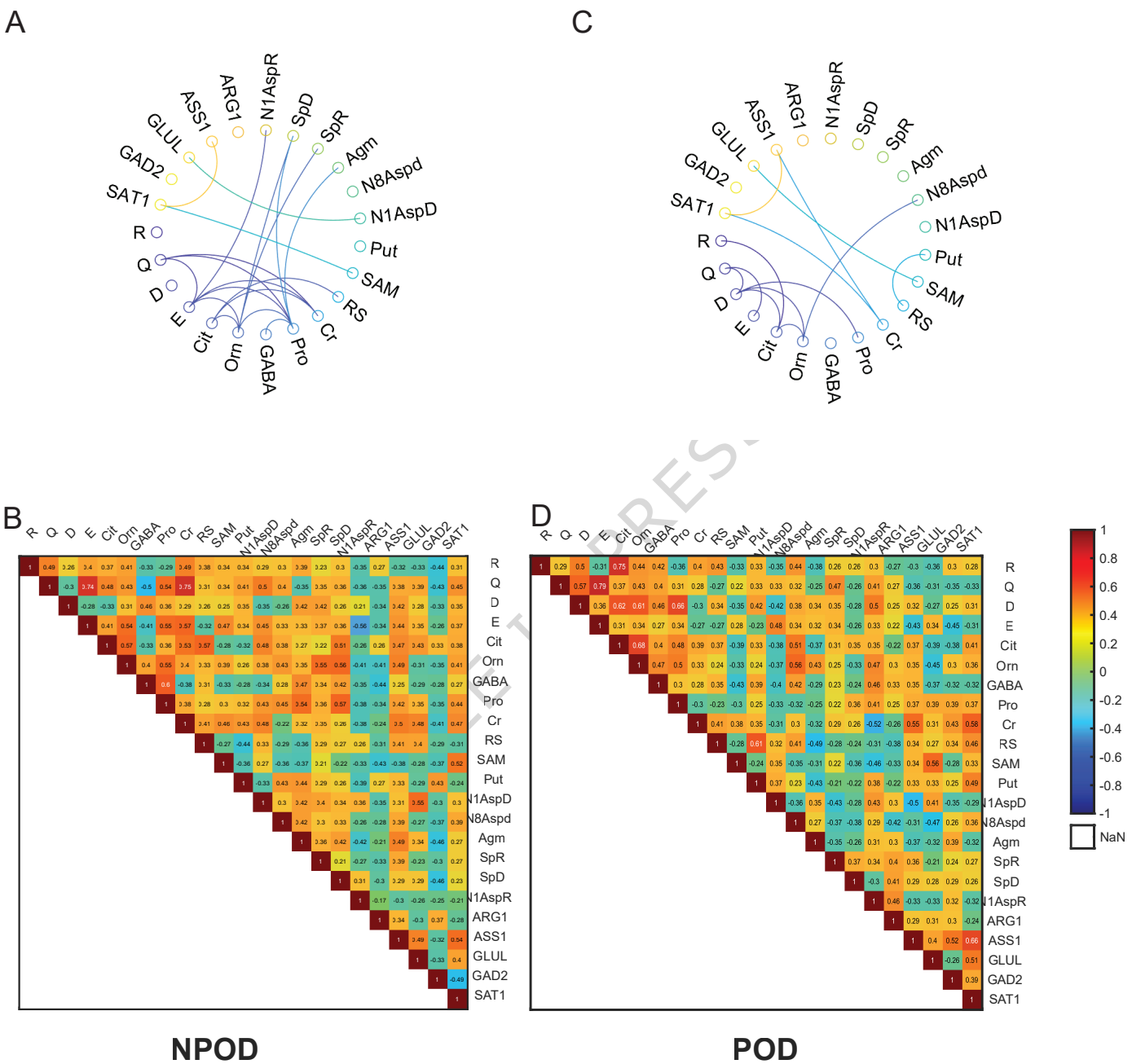
A
ARG1
N1AspR
SpD
SpR
Agm
N8Aspd
N1AspD
Put
SAM
RS
Cr
Pro
GABA
Orn
Cit
E
D
Q
R
SAT1
GAD2
GLUL
ASS1
C
B
D
NPOD
POD
NaN

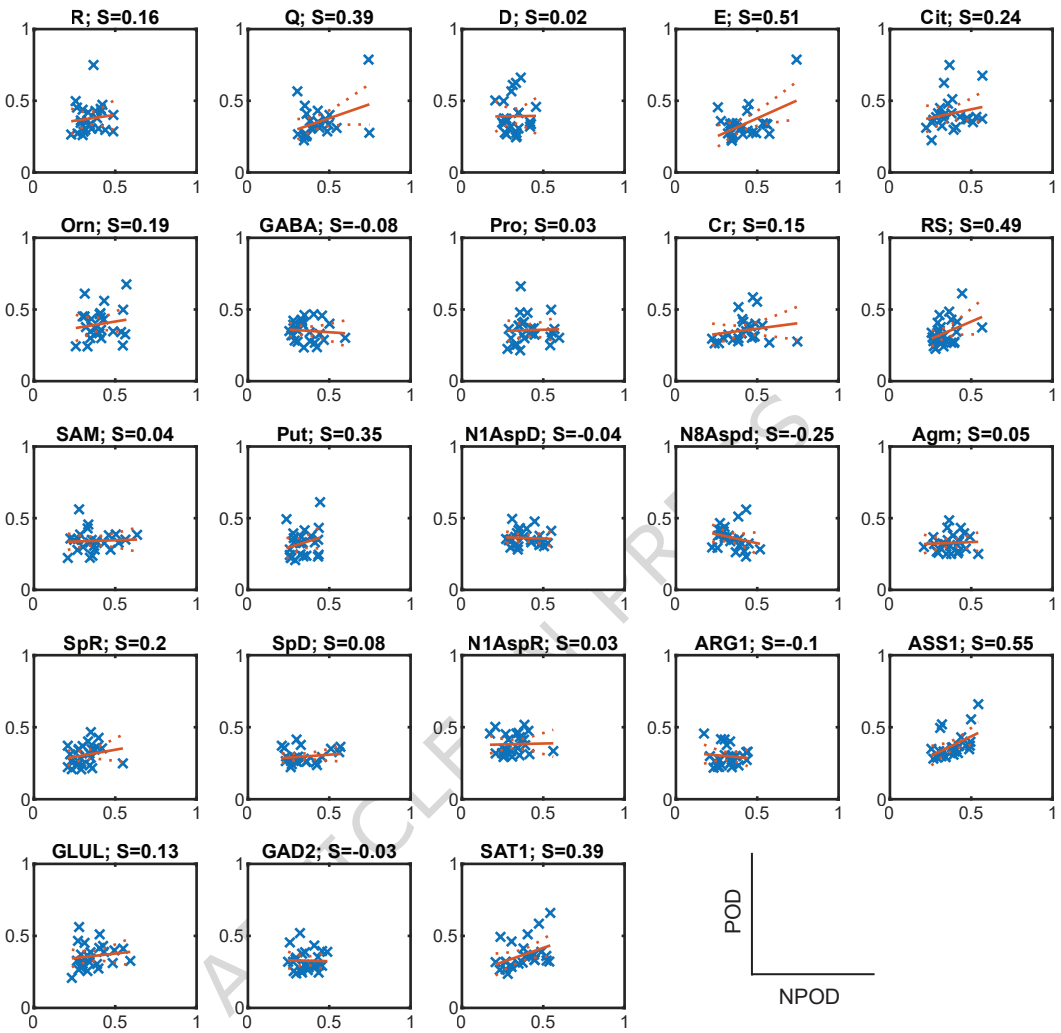

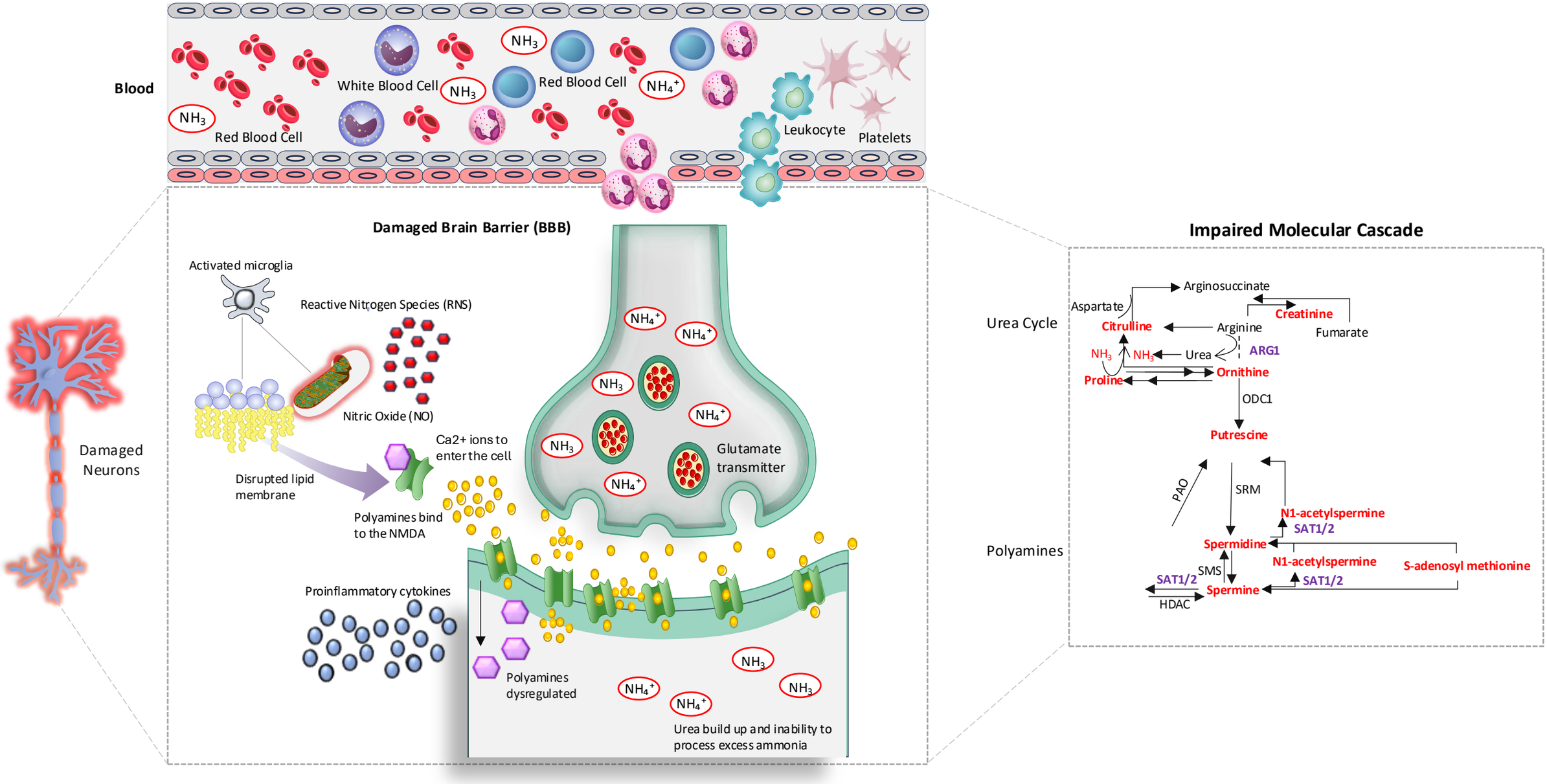
Blood
White Blood Cell
Red Blood Cell
Red Blood Cell
Leukocyte
Platelets
NH3
NH4+
Damaged Neurons
Damaged Brain Barrier (BBB)
Activated microglia
Reactive Nitrogen Species (RNS)
Nitric Oxide (NO)
Disrupted lipid membrane
Ca2+ ions to enter the cell
Polyamines bind to the NMDA
Glutamate transmitter
Proinflammatory cytokines
Polyamines dysregulated
Urea build up and inability to process excess ammonia
Impaired Molecular Cascade
Urea Cycle
Polyamines
Aspartate
Arginosuccinate
Citrulline
Arginine
Creatinine
Fumarate
Urea
ARG1
Proline
Ornithine
ODC1
Putrescine
PAO
SRM
N1-acetylspermine
SAT1/2
Spermidine
SMS
S-adenosyl methionine
Spermine
HDAC